# REPORT ON WORKSHOP: DEFINING RTE SOLUTION METHODS FOR MULTI-MODE TRANSFER

## June 3-4, 2016, Istanbul

## Jack Howell and Pinar Mengüç

### WORKSHOP DESCRIPTION:

Over twenty years ago, a workshop was organized to consider the state of computational ability for radiative transfer, and the radiation energy transfer community was invited to use a favorite method to solve a set of prescribed radiation problems of varying degrees of complexity [1]. Comparison of solutions uncovered significant disagreement among solutions, and pointed to reasons for the disagreement, such as variations in the way that the spectral properties of a medium were treated. This study helped in gaining consensus in the community on the suitability of various methods for treating radiative transfer at the time. Since that study, new methods for treating radiation have emerged, highly parallel computing has become common, and more techniques for accurately treating spectrally dependent properties are available.

A Workshop was held on June 3-4, 2016 in Istanbul to broaden the earlier study to include conjugate energy transfer problems that include major effects of radiative energy transfer based on the present state of research on radiative transfer methods. (Attendees are listed in the Appendix.) Such problems occur across a wide selection of disciplines including aerospace re-entry problems, atmospheric modeling and global warming, bioengineering, thermally-based manufacturing, wildfire propagation, food preparation, combustion, propulsion, astrophysics, and many others.

There is no consensus in the radiative energy transfer community on the best method or methods for numerical solution of radiative transfer in such multi-mode (conjugate) coupled energy transfer/fluids problems. Commercial multi-physics codes include some capability for calculating radiative energy transfer, and various choices of solution methods may be included. The choice among the methods is left to the user. Further, code developers for solution of multi-mode problems in academia, research institutions, national laboratories, and companies desiring to solve practical problems may not be familiar with the known pros and cons that impact the choice among the various radiative transfer solution methods.

The choice of radiative transfer solution method requires consideration of trade-offs among required solution accuracy, computation time, and ease of incorporation into multimode problems (grid compatibility, stability, dimensionality. etc.) The choice of method will also depend upon the radiative properties of the medium involved in a conjugate problem, including the optical thickness (transparent, optically thin or thick), scattering albedo, the need to include anisotropic scattering, and the need to treat spectral properties. The scope of such factors makes the choice of a solution method difficult even for those knowledgeable in the field of radiation, let alone the casual user of commercial codes.

The Workshop was held to investigate and quantify the relative advantages of each method for treating radiative energy transfer. The agenda was to

1) Convene the workshop of academic researchers involved in radiative transfer methodology. The participants considered: a. How to define the important factors and the boundaries (properties, accuracy, computational time, suitability for parallelization, others) that determine the choice of best radiative transfer method.

b. Determining or giving the best advice for determining these boundaries.

c. Formulating a suite of problems that can be used to compare the time/accuracy tradeoff of the various methods for treating radiation in combined mode problems.

d. Discussing how best to disseminate the results of the study and encourage participation in solving some or all the entire suite of problems.

2) Present a report of the findings of the Workshop at the RAD-16 Symposium.

a. Using the results of Task 1c, solicit investigators to submit solutions to the formulated combined mode problems. The solutions will incorporate measures of solution time and accuracy.

b. Contact national and international conference organizers (ASME, AIAA, the International Center for Hear and Mass Transfer, etc.) to provide one or more forums for presenting results of individual solutions to the Task 1c problem set.

c. Gather and compare the information on computation time, solution accuracy and ability to massively parallelize the various techniques.

d. Prepare a summary paper comparing the results of the investigators and the various methods, along with recommendations for best methods to use in various parameter ranges. This will also be presented at one forum of Part 2b, as well as submitted for publication in an appropriate journal, such as JQSRT. A special issue or section of a journal will be solicited to present the papers and summary.

Following are four problems, formulated to exercise radiation solvers employed in conjugate energy transfer problems where radiative transfer is an important component of the total energy transfer. Energy transfer researchers are invited to solve the problems, with special attention to comparisons of accuracy and computation time when using different radiation solvers.

# THE PROBLEM SET

Following are the four problems prepared by the Workshop participants after several face-to-face and on-line discussions. It is hoped that researchers in the numerical radiation transfer community will attempt to solve one or more of the problems, and present their results at technical meetings, for publication in journals, or for posting on the web site ThermalRadiation.net[1] [2]. It is recognized that this problem set does not cover the full range of multi-mode problems that can appear in practice. They do represent cases of practical industrial interest and should provide some useful information on choosing the best solvers for similar problems.

References have been provided with each problem set. Where it is available, experimental data or previous solutions are also referenced. These should not be viewed as the exact or benchmark results, although the problem specifications have been formulated to be quite close to the available systems.

The presented problems are inherently complex, and some involve laminar or turbulent flows, spectral properties of inhomogeneous participating media, possible turbulence-radiation interactions, and others. The Workshop attendees discussed at length whether to impose which models for these effects should be used in the solutions, or whether to leave the choice to the person(s) attacking the problem. The former path has the virtue that only the effects of the choice of radiation solver should affect comparisons among solutions. However, the latter path was chosen, in the hope that information and discussion might be generated not only about the best radiation solver for each problem, but also on the effect of how the choice of the subsidiary models might have influenced the solutions. When problems are approached, solved, and published, it would certainly benefit the heat transfer community at large if the subsidiary models and the reasons for their choice are addressed by the authors, even if conclusions are not complete and concrete.

This long-term effort is expected to benefit future researchers, coders, and engineers faced with solving this class of problems. Additional problems will be added to this challenge in the future by sending a complete problems statement to the authors. They will circulate it to the workshop members for review and comment and added to the present set.

## PROBLEM 1: Free Laminar Flame

### Problem Statement

The objective of this problem is to compute the radiative transfer for a series of non-premixed laminar open flames of $CH_4$/air for which experimental data of radiative heat fluxes can be found in [3]. Although this paper does not report other parameters for the flames, such as the mole concentrations of the main chemical species, the temperature and velocity fields, the measured heat fluxes might be a useful basis for comparison with the numerical simulations. According to the authors, the estimated uncertainties related to the heat flux fall within 5%. The problem geometry was based on a modified Santoro's burner, in which the fuel injection tube was extended the distance $L_1 = 6.40 \times 10^{-2}$ m above the air coflow tube to reduce blocking of the coflow tube in the measurement of the heat flux below in positions below the tip of the fuel tube. This is illustrated in Figure 1. The fuel tube has an inner diameter ($d_{fuel}$) of $1.11 \times 10^{-2}$ m, with a wall thickness of $7.94 \times 10^{-4}$ m. The inner diameter of the air annular coaxial outer tube is $d_{coflow} = 1.02 \times 10^{-1}$ m. As with the standard Santoro burner, both tubes are made of brass. Fuel is injected at different flow rates for the flames designated in [3] by the numbers 2, 4, 9 and 11, according to the average velocities presented in Table 1.

---

The velocity profile of the fuel can be taken as developed (parabolic profile) at the outlet of the tube. In all these cases, the air is injected at a flow rate of 100 l/min; its velocity can be taken at the uniform value of $2.08\times10^{-1}$ m/s. Under these conditions, the flame regime proved to be laminar for all cases. The air composition is 21% oxygen and 79% nitrogen by volume. Both fuel and air are injected at the prescribed temperature of 298 K. The boundaries of the system, including the tube walls, can be treated as black surfaces at the environment temperature of 298 K. The only exception is for the boundary surface at $z = L_3$. The surface that is crossed by the flue gas can be treated as black at the outflow bulk temperature; the remaining annulus surface can be treated as black at the environment temperature, 298 K.

Measurement data can be found in [3] for the radiative heat flux normal to the control surface at $r = R$ and $-L_2 \leq z \leq L_3$. Values of $L_2$ and $L_3$ are presented in Table 1 together with $L_f$, which represents the measured visible length of each flame. Some specific results of interest are the radiative energy source field in the domain as well as the radiative energy flux normal on the control surface for comparison with the experimental data. Since the computation of the radiative transfer in the flame depends on the temperature field as well as the fields of the participating species mole concentrations, it is necessary that each solution clearly specifies the models employed for the solution of all involved phenomena, such as the combustion kinetics.
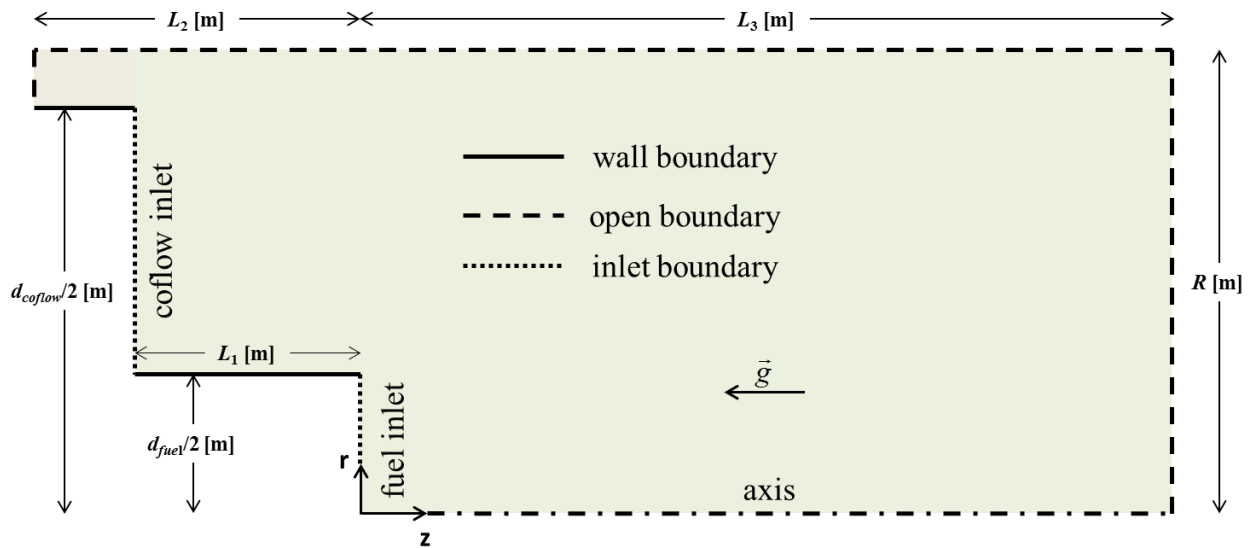


Figure 1 – Domain geometry dimensions and boundaries specification for Problem Set 1.

Because this flame is optically thin, any RTE solver may provide good agreement with the experimental data. Therefore, after solutions are generated for the specified base case, proceed to provide solutions for the case when all radial dimensions are increased by a factor of 4.0. Change the inlet flow rates for fuel and air so that the Reynolds number is the same as for the base case. Provide similar results as for the base case but adjusted for the increased burner diameter. Although experimental results are not available for this larger burner, the radiative emission is much larger, and comparison of solution methods should show more differences.

Table 1 – Fuel inlet velocity for the constant power flame series.

| Flame | Velocity [m/s] | $R$ [m] | $L_f$ [m] | $L_2$ [m] | $L_3$ [m] |
|---|---|---|---|---|---|
| 2 | $5.17\times10^{-2}$ | $0.540\times10^{-2}$ | $5.50\times10^{-2}$ | $0.680\times10^{-2}$ | $1.65\times10^{-1}$ |
| 4 | $6.89\times10^{-2}$ | $0.540\times10^{-2}$ | $7.60\times10^{-2}$ | $0.680\times10^{-2}$ | $2.28\times10^{-1}$ |
| 9 | $1.21\times10^{-1}$ | $1.14\times10^{-1}$ | $1.39\times10^{-1}$ | $1.38\times10^{-1}$ | $4.17\times10^{-1}$ |
| 11 | $1.55\times10^{-1}$ | $1.14\times10^{-1}$ | $1.89\times10^{-1}$ | $1.38\times10^{-1}$ | $5.67\times10^{-1}$ |

Source: adapted from [3].

## PROBLEM 2: Free Turbulent Flame

**Problem Statement**

The objective of this problem is to compute the radiative transfer in the non-premixed turbulent flame DLR-A which was measured in [4 to 6]. Figure 2 presents a schematic of the burner, which consists of a coflow configuration of fuel, in the inner tube, and air, in the outer tube. The burner is aligned with the vertical direction, but for convenience it is shown in the horizontal position in the figure. The fuel mole concentration composition is $Y_{CH4} = 0.221$, $Y_{H2} = 0.332$ and $Y_{N2} = 0.447$. The fuel tube inner diameter is $d = 8.0$ mm. The velocity of the jet is 42.15 m/s, resulting in $Re_d = 15200$. The air coflow has a velocity of 0.3 m/s, temperature of 292 K, and its mole concentration composition $Y_{O2} = 0.208$, $Y_{N2} = 0.784$ and $Y_{H2O} = 0.008$. The environment temperature is 292 K. For this flame, the adiabatic flame temperature is $T_{ad} = 2130$ K. For the geometrical domain it can be considered that the inner and outer tubes have a length of 40 cm; at the inlet of the tubes, the fuel and air velocities can be assumed uniform. For the simulation, it is recommended a computational domain with length of 200 cm and diameter of 80 cm, as seen in the figure. The boundaries of the system, including the tube walls, can be treated as black surfaces at the environment temperature. The only exception is for the boundary surface at $x = 200$ cm. The surface that is crossed by the flue gas can be treated as a black surface at the outflow bulk temperature; the remaining annulus surface can be treated as a black at the environment temperature.

Results of the global simulation of the flame results can be compared with experimental data in [4], which includes the temperature and mole concentrations of $N_2$, $O_2$, $CO_2$, $H_2O$, $H_2$, CO, OH, and NO along the flame axis ($2.5 \leq x/d \leq 120$) and radial directions (for $x/d = 5$, 10, 20, 40, 60, 80), including both mean and rms values. In addition, measurements of line-of-sight spectral radiation intensities and statistical data can be found in references [5] and [6].
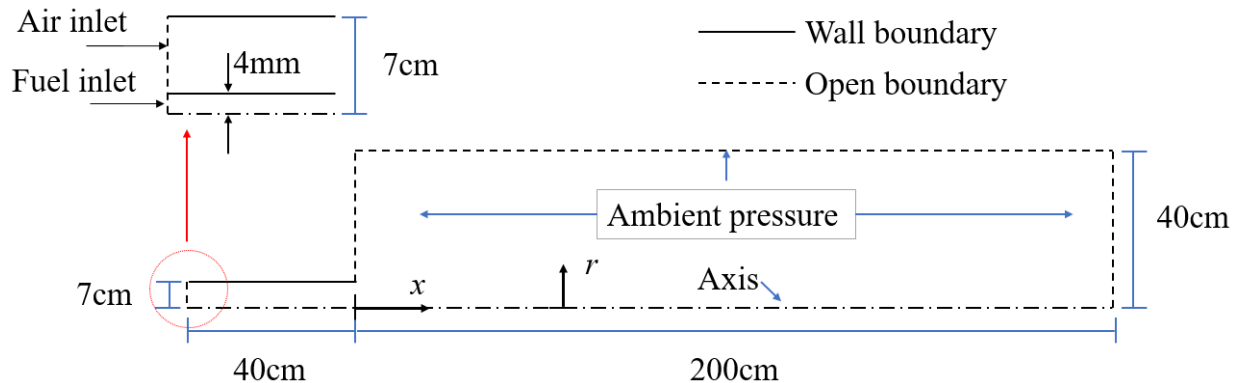


Figure 2. Geometrical domain and boundary conditions for Problem Set 2.

The computation of the radiative transfer in the flame depends on the temperature field as well as the fields of the participating species mole concentrations. To allow the reproduction of the numerical solutions, it is necessary that each solution clearly specifies the models employed for the solution of all involved phenomena, such as the turbulent transport (including turbulence-radiation interactions) and combustion kinetics.

Some specific results of interest for the radiative energy transfer are the radiative energy source field in the domain as well as the radiative energy flux normal to the side control surface, that is, for $0 \leq x \leq 200$ cm and $r = 40$ cm. It is necessary to provide all information regarding the methods employed for both the spatial and spectral integration of the radiative transfer, including the effects of turbulence-radiation interactions (TRI).

Because this flame is optically thin, any RTE solver may provide good agreement with the experimental data. Therefore, after solutions are generated for the specified base case, proceed to provide solutions for the case when all radial dimensions are increased by a factor of 4.0. Change the inlet flow rates for fuel and air so that the Reynolds number is the same as for the base case. Provide similar results as for the base case but adjusted for the increased burner diameter. Although experimental results are not available for this larger burner, the radiative emission is much larger, and comparison of solution methods should show more differences

## PROBLEM 3:  High Temperature Porous Medium

**Problem Statement**

Multimode energy transfer in a catalytic reticulate porous ceramic (RPC) exposed to direct high-flux directional irradiation is considered.  The RPC is used for steam reforming of methane and it is saturated with reacting gas flow.  The problem considered here is originally presented in [7], along with its solution and it represents the typical operating conditions of a solar reforming system.

The thickness of the RPC is 4 cm, and it is smaller compared to horizontal and vertical dimensions so that it can be considered as 1D as shown in Fig. 3.  The parameters defining the problem in Fig. 3 are presented in Table 2.  Inlet side radiation boundary condition can be depicted by cold, black surroundings ($T_{surr} = 0$ K), whereas the outlet radiation boundary condition can be considered as perfect diffuse reflection that is equivalent to an adiabatic boundary condition.  The nominal RPC pore size ($d_{nom}$) is 2.54 mm (10 ppi foam) with a porosity $\varepsilon = 0.911$ (Type 1) or 0.858 (Type 2).
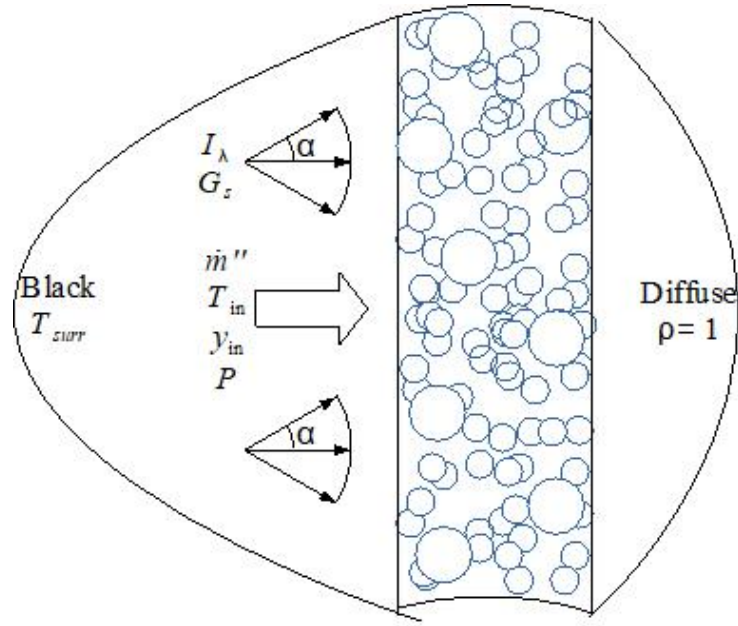
Figure 3 The geometry for Problem 3 showing the sketch of the 1D RPC that is used for steam reforming of methane and subject to high intensity directional solar flux.

Table 2:  Boundary conditions for 1D RPC.

| $\dot{m}''$ | 0.9 kg/m²s |
|---|---|
| $y_{H2O,in}/y_{CH4,in}$ | 2 |
| $T_{in}$ | 800 K |
| $P$ | 5 bar |
| $G_s$ | 500 kW/m² |
| $\alpha$ | 25° |

Radiative Properties:

The gas can be considered as non-participating based on the low Planck mean absorption coefficients for $CH_4$ and $H_2O$ at 800 K. For incident radiation of blackbody spectral distributions of 5870 K and 1100 K, the latter representing reactor's wall. The calculated absorption coefficients are negligible with respect to the extinction coefficient of the RPC. Therefore, the gas phase can be considered transparent, whereas the extinction coefficient of the RPC can be defined by the following correlation:

$$\beta = \frac{5.5173}{d_{nom}}(1-\varepsilon)$$

(1)

The RPC is coated with a catalyst that is supported by a rough microscopic wash-coating and the reflection from the RPC surface can be approximated as diffuse. The scattering phase function can be represented with the following simple expression, presented as a polynomial as:

$$\Phi(\mu) = \sum_{i=0}^{5} a_i \mu^i \qquad (2)$$

where $a_0$=0.8044, $a_1$=-1.4116, $a_2$=0.5619, $a_3$=0.0052, $a_4$=0.0420, and $a_5$=-0.0055.

Effective Thermal Conductivity and Permeability:

The effective thermal conductivity of fluid-saturated RPC can be predicted from high resolution computer tomography (CT) based numerical analysis [8], using both macro and micro-scale analyses. The macro-scale analysis relates the ratio of effective conductivity of the RPG to effective thermal conductivity of the strut structure, $k_{e,RPG}/k_{e,strut}$, as a function of the ratio of the fluid-to-strut thermal conductivities, $k_f/k_{e,strut}$. Similarly, the micro-scale analysis relates the ratio of the effective thermal conductivity of strut structure to thermal conductivity of the solid phase, $k_{e,strut}/k_s$, to the fluid to solid thermal conductivity ratio, $k_f/k_s$. The effective thermal conductivity of RPC is defined as a superposition of these two effects as:

$$\frac{k_{e,RPC}}{k_s} = \left(\frac{k_{e,RPC}}{k_{e,strut}}\right)\left(\frac{k_{e,strut}}{k_s}\right) \qquad (3)$$

It is shown that the upper bound correlation proposed by Miller [9] represents both ($k_{e,RPC}/k_{e,strut}$) and ($k_{e,strut}/k_s$), quite accurately, with a root mean square error of 3.6% and 0.184%, respectively [8]. The upper bound correlation as defined by Miller can be represented as:

$$k_r = v\left\{1+(1-\varepsilon)\left(\frac{1}{v}-1\right)-\left(\frac{\frac{1}{3}\varepsilon(\varepsilon-1)\left(\frac{1}{v}-1\right)^2}{1+\left(\frac{1}{v}-1\right)\left[(1-\varepsilon)+3\left(\varepsilon^2 G_1 - (1-\varepsilon)^2 G_2\right)\right]}\right)\right\} \qquad (4)$$

where, $G_1$=0.1508 and $G_2$=0.1111 for $k_r=k_{e,RPC}/k_{e,strut}$, $v=k_f/k_{e,strut}$; and $G_1$=0.1287 and $G_2$=0.2157, for $k_r=k_{e,strut}/k_s$, $v=k_f/k_s$.

The permeability of the structure can be defined based on direct pore-level numerical simulation and it was found in [10] that the inverse dimensionless permeability ($c_0=d_{nom}^2/K$) and the dimensionless Dupuit–Forchheimer coefficient ($c_1=d_{nom}F$) are estimated to be 49.7 and 1.128, respectively.

Benchmark Results:

The multi-mode problem is to be solved considering conduction, convection and radiative transfer through the porous medium. Fluid mechanics are governed by the Dupuit-Forchheimer equation, ignoring the Brinkmann viscous term. The Langmuir-Hinshelwood model can be used for modeling steam reforming as it is found to approximate the experimental results more accurately than others [7].

The temperature of solid phase, temperature of the fluid phase, the solid-fluid energy transfer rate, molar fraction of the species, the pressure drop is to be predicted along the 1D medium.

## PROBLEM 4: Steel Reheating Furnace

**Problem Statement**

Due to its high consumption of fossil energy and environmental restrictions, there is a major interest in the optimization of the design and operation of the thermal processes in the steel industry. One of the main thermal systems in the steel industry is the reheating furnace, in which the steel, usually in the form of billets or slabs, is introduced to be heated to a certain temperature, as needed by subsequent processes. Computational simulation is a fundamental tool to optimize the design of such furnaces, for instance to reduce emission of pollutants and greenhouse gases or to attain uniformity of heating of the steel. Due to the high complexity of the phenomena involved in the process, engineers and researchers usually rely on the use of commercial CFD codes, either using the available models or combining them with user-defined functions to include specific requirements [11 to 14].

The objective of this problem is to solve the energy transfer combining turbulent convection and radiation in participating medium in a typical industrial billet reheating furnace. The system configuration is presented in Fig. 4. The furnace has rectangular shape, with the main dimensions indicated in Fig. 5, and specified in Table 3. There is a total of 24 radiant burners distributed in two zones: heating zone 1, with 15 burners, and heating zone 2, with 9 burners. To stabilize and shape the flame, the fuel (methane) and air injection are placed in the interior of refractory tiles, as seen in Fig. 6. The exit surface of each tile is at the same level of the top surface of the furnace (Fig. 6). As a common practice in the furnace operation, the flame length is reduced due to the swirl generated by the air inflow, so that the flame is fully contained inside the tile. Thus, it can be considered that only a flue gas jet crosses the tile exit surface. With this assumption, this problem can be solved without the need to solve the combustion kinetics in the burners, and the focus is the energy transfer combining radiation and convection in a complex turbulent flow field. Considering stoichiometric combustion of methane in atmospheric conditions, the flue gas jet can be treated as a homogeneous mixture of $H_2O$ (0.2 atm), $CO_2$ (0.1 atm) and $N_2$ (0.7 atm), which can be considered the same composition of the furnace internal medium. In steady state conditions, the flue gas entering the furnace through the 24 burners exits the furnace through an exhaust duct with a rectangular entrance, which is placed on the top surface of the furnace (Fig. 4).

The mass flow rate of the flue gas in each burner of the heating zones 1 and 2 are $\dot{m}_1 = 0.25$ kg/s and $\dot{m}_2 = 0.15$ kg/s, respectively. The total mass flow rate in the furnace is therefore 5.1 kg/s. The temperature of the flue gas jet leaving all burners (zones 1 and 2) is $T_g = 2000$ K.

Regarding the boundary conditions, the furnace can be divided in four types of surfaces: the bottom surface, representing the billets in motion; the exit surfaces of the tiles containing the flue gas jets; the inlet surface of the exhaust duct; and the remaining walls. The necessary conditions are the following:

(i) Bottom surface. The billets are heated from the inlet temperature $T_{in} = 300$ K to $T_{out} = 1400$ K as they move along the bottom of the furnace. For simplification, the bottom surface of the furnace can be assumed to be perfectly flat, with a continuous variation of the temperature in the $x$-direction according to the exponential relation below:

$$T(x) = T_g - (T_g - T_{in})\exp(-Cx/L_1) \tag{5}$$

where the constant $C$ is $\ln[(T_g - T_{in})/(T_g - T_{out})]$. The position $x$ starts on the right side of the furnace (Fig. 5), varying between $0 \leq x \leq L_1$. Temperature variations in the $y$-direction can be neglected in the present problem. The bottom surface can be assumed perfectly diffuse and gray with emissivity $\varepsilon_{bs} = 0.7$.

(ii) The tile exit surface. The temperature of the flue gas jet and of the surface is $T_g$. For the radiative transfer analysis, the entire exit surface of the tile can be treated as a black surface at the temperature $T_g$. It can be considered that the flue gas jet has constant velocity profile in the $z$-direction, which is normal to the exit surface. Figure 6 shows the axial velocity $u_z$ with negative signal, since its direction is opposite to the $z$-direction. (It follows from this that $u_z$ is a positive quantity.) The axial velocities can be directly computed from the specified mass flow rate in each burner ( $\dot{m}_1$ for burners in the heating zone 1, or $\dot{m}_2$ for heating zone 2). To account for the swirl generated in the burner, an azimuthal velocity $u_\theta$ can be imposed by the following relation:

$$u_\theta = 2Sru_z / R \tag{6}$$

where $S$ is the swirl number. To study the effect of the swirl number, it is suggested to set the following conditions: $S = 0.1$, 0.2 and 0.3. The jets can also be assumed turbulent with turbulence intensities of 10% for the jets in the heating zones 1 and 2, respectively.

(iii) Exhaust duct entrance surface. Outflow conditions can be set for the rectangular surface representing the entrance of the exhaust system. For the radiative calculation, the surface can be treated as a black surface at the bulk temperature of the gas exiting the furnace. This will require an iterative solution.

(iv) Furnace walls. The remaining walls of the furnace can be assumed to be adiabatic. This will allow decoupling the energy transfer in the interior of the furnace, the focus of this problem, of the energy transfer in the outside environment. The wall surfaces can be considered perfectly diffuse and gray with emissivity $\varepsilon_{ws} = 0.9$.

Some specific results of interest are the total, the radiative and the convective energy fluxes distribution on the bottom surface of the furnace. It is necessary to provide all information regarding the methods employed for both the spatial and spectral integration of the radiative transfer as well as the models for the solution of the turbulent flow in the furnace. Variation of the properties for the gas mixture with the temperature should be considered.
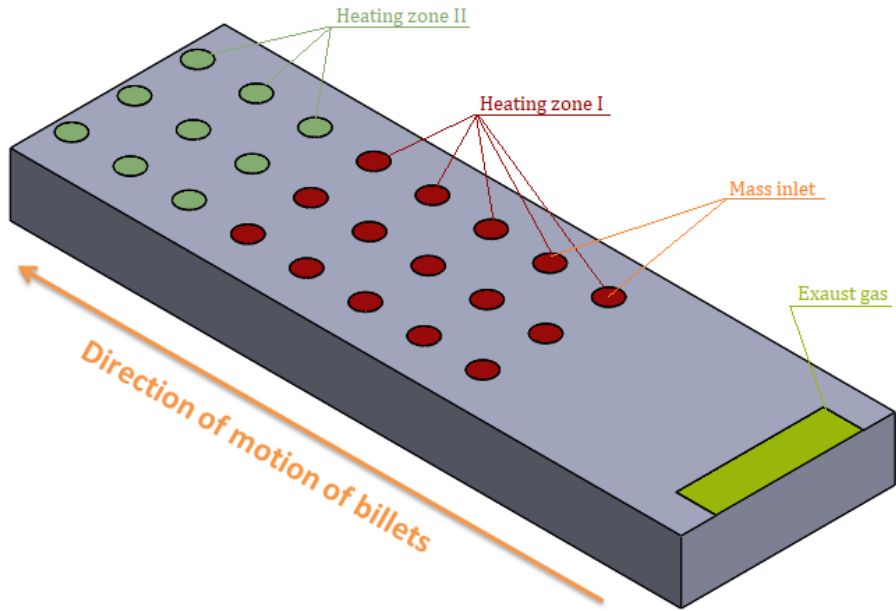
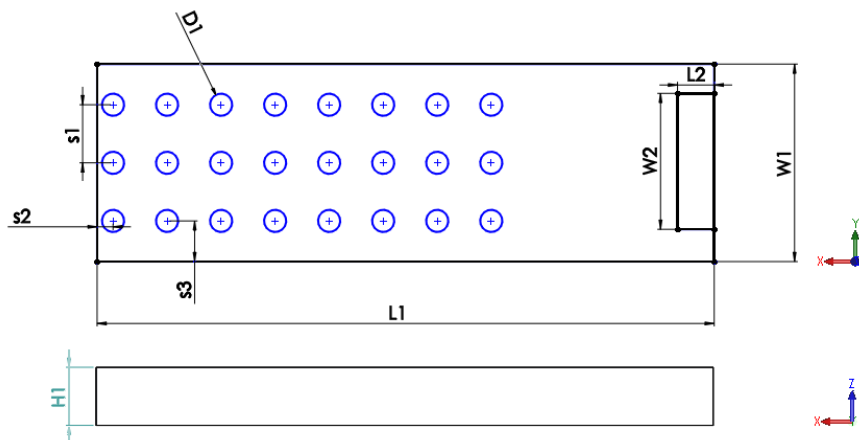Fig. 4 – Representation of a typical billet reheating furnace for Problem 4.



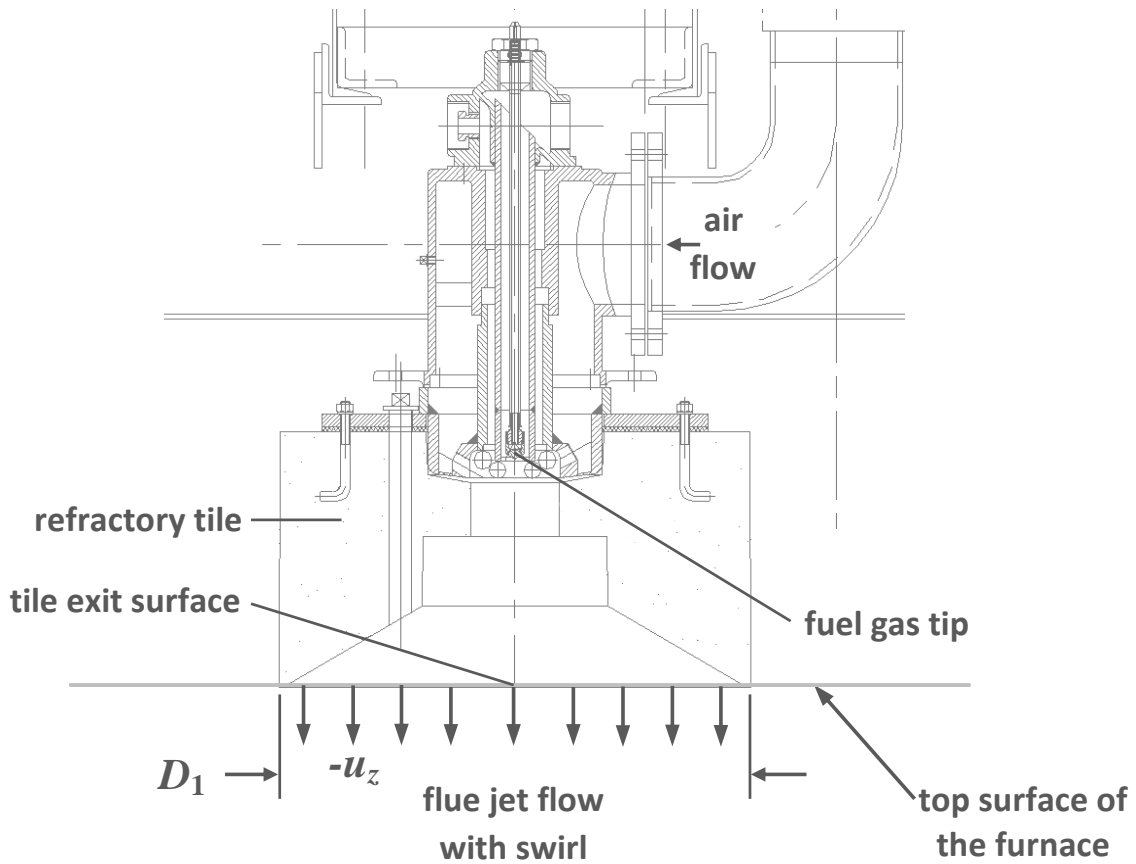Fig. 5 – Upper and side view of the furnace with the main dimensions.

Fig. 6 – Details of the burner and the representation of the flue jet flow through the tile exit surface.

Table 3 – Values and descriptions of the furnace main dimensions.

| Dimension | Description | Value |
|---|---|---|
| $L_1$ | Length of the furnace | 16.0 m |
| $L_2$ | Length of the entrance of the exhaust duct | 0.950 m |
| $W_1$ | Width of the furnace | 5.10 m |
| $W_2$ | Width of the entrance of the exhaust duct | 3.15 m |
| $H_1$ | Height of the furnace | 1.50 m |
| $D_1$ | Diameter of the tile exit surface | 0.575 m |
| $D_2$ | Effective diameter of the flue gas jet | 0.173 m |
| $s_1$ | Spacing between the burners in the $x$ and $y$-direction | 1.40 m |
| $s_2$ | Spacing between the side wall and the closest burners ($x$-direction) | 0.480 m |
| $s_3$ | Spacing between the side walls and the closest burners ($y$-direction) | 1.05 m |

# REFERENCES

[1] Tong, T. W., and Skocypec, R. D., Summary on Comparison of Radiative Heat Transfer Solutions for a Specified Problem, *ASME HTD-vol. 203*, pp. 253-264, 1992.

[2] Howell, J.R., Mengüç, M.P., Depository of Challenge Problems and Solutions, at Thermalradiation.net, http://www.thermalradiation.net, 2018.

[3] Miguel, R.B., Machado, I.M., Pereira, F.M., Pagot, P.R., França, F.H.R. "Application of inverse analysis to correlate the parameters of the weighted-multi-point-source model to compute radiation from flames", Int. J. Heat Mass Trans., **102**, 816-825, 2016.

[4] Sandia National Laboratories. "International workshop - measurements and computations of turbulent nonpremixed flames - CH4/H2/N2 jet flames". http://www.sandia.gov/TNF/DataArch/DLRflames.html

[5] Zheng Y, Sivathanu YR, Gore JP. Measurements and stochastic time and space series simulations of spectral radiation in a turbulent non-premixed flame. Proc Combust Inst 2002; **29:1957**–63.

[6] Zheng Y, Barlow RS, Gore JP. Measurements and calculations of spectral radiation intensities for turbulent non-premixed and partially premixed flames. J Heat Transfer 2003; **125:678**–86.

[7] Petrasch J.: "Multi-scale analyses of reactive flow in porous media." ETH Zurich, 2007. doi.org/10.3929/ethz-a-005397926

[8] Petrasch J., Schrader B., Wyss P., Steinfeld A.: "Tomography-Based Determination of the Effective Thermal Conductivity of Fluid-Saturated Reticulate Porous Ceramics." J Heat Transfer 2008; **130:32602**. doi.org/10.1115/1.2804932

[9] Miller M.N.: "Bounds for Effective Electrical, Thermal, and Magnetic Properties of Heterogeneous Materials." J Math Phys 1969; **10:**1988–2004. doi.org/10.1063/1.1664794

[10] Petrasch J., Meier F., Friess H., Steinfeld A.: "Tomography based determination of permeability, Dupuit-Forchheimer coefficient, and interfacial heat transfer coefficient in reticulate porous ceramics." Int J Heat Fluid Flow 2008; **29**:315-326. doi.org/10.1016/j.ijheatfluidflow.2007.09.001

[11] Han, S. H.; Chang, D.; Kim, C. Y.; "A numerical analysis of slab heating characteristics in a walking beam type reheating furnace", Int. J. Heat Mass Transfer **53**, 3855-3861, 2010.

[12] Han, S. H.; Chang, D.; "Optimum residence time analysis for a walking beam type reheating furnace", Int. J. Heat Mass Transfer **55**, 4079-4087, 2012.

[13] Mayr, B.; Prieler, R.; Demuth, M.; Moderer, L.; Hochenauer, C.; "CFD Analysis of a pusher type reheating furnace and the billet heating characteristic", Applied Thermal Engineering **115**, 986-994, 2017.

[14] Prieler, R.; Mayr, B.; Demuth, M.; Holleis, B.; Hochenauer, C.; "Prediction of the heating characteristic of billets in a walking hearth type reheating furnace using CFD", Int. J. Heat Mass Transfer **92**, 675-688, 2016